Projection Method for the Hankel Transform

Andrey S. Krylov Maxim M. Mizotin

11 июня 2011 г.

Аннотация

Numerical projection method for the zero-order Hankel transform inversion for the case of the data given on a finite interval has been developed. The justification of the convergence of the projection method has been done for the general case that also includes the sine-Fourier transform inversion. An inequality on the norms of the zeroth order Laguerre functions has been proved. Efficiency of the method was illustrated with the test data and for the problem of cylindrical distribution function calculation using melt surface layer diffraction data.

1 Introduction

The Hankel transform is widely used in optics [1, 7], hydrodynamics [2, 9], acoustics [3], image processing [16], etc. The Hankel transform is often used to solve axially symmetric problems in Fourier analysis. In this case, the problem dimensionality can be lowered and the zero-order Hankel transform is used:

$$H\left[z(t)\right] = \int_0^\infty z(x) J_0(xt) x\, dx.$$

Usually the inversion of the Hankel transform is considered for the case

$$H\left[z\right] = u, \quad H : L_2\left[0, \infty\right) \to L_2\left[0, \infty\right).$$

Nevertheless, in practical problems the right part u of this equation (the experimental data) is known only on a finite interval. Thus, instead of the original well-posed inverse problem on a whole half-line we solve an ill-posed inverse problem for the equation

$$H\left[z\right] = u, \quad H : L_2\left[0, \infty\right) \to L_2\left[0, a\right]. \tag{1}$$

Usually the finite Hankel transform is used to solve this problem [15]. Here we have two difficulties. First, the inversion of the Hankel transform on a finite interval is an ill-posed problem. Second, we must assume that the right part and the solution are finite in this case. It is fulfilled only for zero function if we still consider the problem as the Hankel transform inversion problem.

Moreover, due to the ill-posedness of the problem, known analytical formulae of inversion do not provide satisfactory accuracy [5].

An alternative way is to expand the given function into a series of orthonormal eigenfunctions of the Hankel transform. These functions are in fact the Laguerre

functions. Once the function expansion is known, one can easily evaluate its Hankel transform using the obtained expansion coefficients. However, numerical study of the method revealed some details which should be taken in account [18]. The Laguerre functions appreciably differ from zero only on a finite interval (we call it as "numerically concentrated"). The experiments showed that the expansion convergence slows down significantly when this interval goes beyond the region where the data is given. The authors propose an estimate for the "optimal" number of terms in expansion depending on the scale of the Laguerre functions and on the length of the given data interval.

In [14] the numerical concentration property was used in conjunction with the *a priori* knowledge of numerical concentration interval of the solution. The scale for the Laguerre functions was chosen taking into account the concentration domains of both the data and the solution. This allowed to solve the problem without additional proposition on the zero continuation of the right part of the equation (1).

In this paper we propose computational projection method for the case of noisy data given on a finite interval. The convergence of the method is theoretically proved and the optimal number of functions is determined, depending on the interval length and the noise level.

2 The general problem statement and the related works

Consider the general problem of inversion of the integral transform A on a half-line

$$Az = u, \quad A : L_2\,[0,\,\infty) \to L_2\,[0,\,\infty). \tag{2}$$

Usually, the exact right part $\overline{u} \in L_2\,[0,\,\infty)$ is unknown and only the function u_a^δ and the error norm δ are given. Thus the inverse problem is defined by the equations

$$Az = u_a^\delta, \quad A : L_2\,[0,\,\infty) \to L_2\,[0,\,a], \tag{3}$$

$$u_a^\delta \in L_2\,[0,\,a] : \left\|u_a^\delta - \overline{u}\right\|_{L_2[0,\,a]} \le \delta. \tag{4}$$

The problem (3) is ill-posed because its solution is not unique.

The Sine-Fourier transform operator in the case when data is given on a finite interval is the most frequently considered problem of this type [4, 8, 19]:

$$Sz = \int_0^\infty z(y)\sin(xy)\,dy = u_a^\delta(x), \quad S : L_2\,[0,\,\infty) \to L_2\,[0,\,a]. \tag{5}$$

There are two major groups of methods used to solve this problems. The first one uses the zero continuation of u_a^δ to the half-line (we call it "the standard method"). The second one reduces the original problem to the Fredholm equation of the first kind by changing the integration limit to a finite value and applies regularization techniques. The major drawback of the first method is so called "tear effect", while the second group does not use properties of the transform on the whole half-line, thus losing important information about the initial well-posed problem.

In [11,13] the computational projection method was suggested, which combines the regularization technique and the use of the integral transform properties. It

also takes into account the length of the interval where the data is given. This method was successfully applied for solution of the problem (5).

In this work the computational projection method theory is further developed. The new general convergence theorem is proved. It generalizes the result of [11] for the case of noise addition (4) to the right part of (3). The projection method is applied to the numerical solution of the problem (1).

3 Computational projection method of the integral transform inversion

We consider the inverse problem (2). Let the operator A has a full, orthonormal in $L_2\,[0,\,\infty)$ system of eigenfunctions $\{\varphi_i\}$, and the eigenvalues $\{\lambda_i\}$ are finite and isolated from zero:

$$\infty > |\lambda_i| > \lambda > 0. \tag{6}$$

Then the exact right part can be expanded in a Fourier series using the system of eigenfunctions

$$\overline{u}(x) = \sum_{i=0}^{\infty} c_i \varphi_i(x), \quad c_i = \int_0^{\infty} \overline{u}(x)\varphi_i(x)\,dx,$$

and the exact solution $\overline{z}$ is given by:

$$\overline{z}(y) = \sum_{i=0}^{\infty} d_i \varphi_i(y), \quad d_i = \frac{c_i}{\lambda_i}.$$

To solve numerically the problem (3), (4) we construct the projection method using the system of eigenfunctions of the well-posed problem (2). Denote

$$z_a^{\delta}(y) = \sum_{i=0}^{N-1} d_i^{a,\delta} \varphi_i(y), \tag{7}$$

$$d_i^{a,\delta} = \frac{c_i^{a,\delta}}{\lambda_i} = \frac{1}{\lambda_i} \int_0^a u_a^{\delta}(x)\varphi_i(x)\,dx, \quad i = \overline{0, N-1}, \tag{8}$$

where N is the number of terms in the Fourier series expansion.

One of the key points of the projection method is the choice of the number N. In most cases, when no *a priori* information about function $z_a^{\delta}(x)$ is available, the number N is taken as the minimal value, that gives an approximation error of $u_a^{\delta}(x)$ lower than δ. But this choice of N has a drawback because it does not take into account the value of a. When δ is small we need a large N to approximate $u_a^{\delta}(x)$, and if a is finite, the coefficients c_i and $c_i^{a,\delta}$ can differ significantly for large i. Thus we find N as the maximal value of n that satisfies the condition

$$\|\varphi_i\|_{L_2[a,\,\infty)} \le \frac{K_1}{\sqrt{n}}, \quad i = \overline{0, n-1}, \quad \text{and} \quad K_1 > 0 \text{ is a constant.} \tag{9}$$

It selects functions $\varphi_i(x)$, that are numerically concentrated on the interval $[0,\,a]$.

In practice it is important to take into account simultaneously the measurement error value δ and the interval length a to choose N. It can be done using the following theorem:

Theorem 3.1. *Let eigenvalues λ_i of the full, orthonormal in $L_2\,[0,\,\infty)$ system of eigenfunctions $\{\varphi_i\}$ of the operator A (3) satisfy the condition (6) and the eigenfunctions are ordered so that:*

$$\|\varphi_i\|_{L_2\,[a,\,\infty)} \le \|\varphi_{i+j}\|_{L_2\,[a,\,\infty)}\,, \quad i = \overline{0,\infty}\,,\ j = \overline{k,\infty}\,,\ \forall\, a > 0,\ k \in \mathbb{N}. \tag{10}$$

Let

$$N_a = \max\left\{n \in \mathbb{N} : \|\varphi_{n-1}(x)\|_{L_2[a,\infty)} \le \frac{K_1}{\sqrt{n}}\right\}, \quad K_1 \in (0,1], \tag{11}$$

$$N_\delta = \min\left\{n \in\ \mathbb{N} : \left\|\tilde{u}_a^\delta(x) - u_a^\delta(x)\right\|_{L_2[0,a]} \le K_2\delta\right\}, \quad K_2 > 0, \tag{12}$$

where $\tilde{u}_a^\delta = Az_a^\delta$. If

$$N = \min\left\{N_\delta, N_a\right\},\ \textit{then} \tag{13}$$

$$\left\|z_a^\delta - \overline{z}\right\|_{L_2[0,\infty)} \underset{\substack{\delta\to 0\\ a\to\infty}}{\longrightarrow} 0, \tag{14}$$

$$\textit{and} \quad \left|d_i^{a,\delta} - d_i\right| \le \frac{1}{|\lambda_i|}\left(\delta + \frac{K_1}{\sqrt{N_a}}\,\|\overline{u}\|_{L_2[a,\infty)}\right) \quad \textit{for} \quad i < N_a. \tag{15}$$

Доказательство. The estimate (15) can be obtained using Hölder inequality for the right part of

$$\left|d_i^{a,\delta} - d_i\right| = \frac{1}{|\lambda_i|}\left|\int_0^a u_a^\delta(x)\varphi_i(x)\,dx - \int_0^\infty \overline{u}(x)\varphi_i(x)\,dx\right| \le$$

$$\le \frac{1}{|\lambda_i|}\left(\left|\int_0^a (u_a^\delta(x) - \overline{u}(x))\varphi_i(x)\,dx\right| + \left|\int_a^\infty \overline{u}(x)\varphi_i(x)\,dx\right|\right)\,.$$

Then,

$$\left|d_i^{a,\delta} - d_i\right| \le \frac{1}{|\lambda_i|}\left(\|\overline{u}(x) - u_a^\delta(x)\|_{L_2[0,\,a]}\|\varphi_i(x)\|_{L_2[0,\,a]} + \right.$$

$$\left. + \|\overline{u}(x)\|_{L_2\,[a,\,\infty)}\|\varphi_i(x)\|_{L_2\,[a,\,\infty)}\right) \le$$

$$\le \frac{1}{|\lambda_i|}\left(\delta + \|\overline{u}(x)\|_{L_2\,[a,\,\infty)}\frac{K_1}{\sqrt{N_a}}\right).$$

Let

$$u^\delta(x) = \begin{cases} u_a^\delta(x), x \in [0,\,a], \\ \overline{u}(x), x > a, \end{cases} \qquad c_i^\delta = \int_0^\infty u^\delta(x)\varphi_i\,dx$$

and z^δ is the corresponding solution of the equation (2). Consider the approximation error:

$$\left\|z_a^\delta - \overline{z}\right\|_{L_2\,[0,\,\infty)} \le \left\|z_a^\delta - z^\delta\right\|_{L_2\,[0,\,\infty)} + \left\|z^\delta - \overline{z}\right\|_{L_2\,[0,\,\infty)}.$$

The second term converges to zero when $\delta \to 0$. It is necessary to show that $\left\|z_a^\delta - z^\delta\right\|_{L_2\,[0,\,\infty)}$ also converges to zero when $\delta \to 0$ and $a \to \infty$.

If $N = N_\delta$, then

$$\left\|z_a^\delta - z^\delta\right\|^2_{L_2\,[0,\,\infty)} \le \frac{1}{\lambda^2}\left\|\tilde u_a^\delta - u^\delta\right\|^2_{L_2\,[0,\,\infty)} = \frac{1}{\lambda^2}\left(\left\|\tilde u_a^\delta - u_a^\delta\right\|^2_{L_2[0,\,a]} + \right.$$
$$\left. + \left\|\tilde u_a^\delta - \overline{u}\right\|^2_{L_2\,[a,\,\infty)}\right) \le \frac{1}{\lambda^2}\left((K_2\delta)^2 + 2\left\|\tilde u_a^\delta\right\|^2_{L_2\,[a,\,\infty)} + 2\left\|\overline{u}\right\|^2_{L_2\,[a,\,\infty)}\right).$$

The value $\left\|\tilde u_a^\delta\right\|^2_{L_2\,[a,\,\infty)} + \left\|\overline{u}\right\|^2_{L_2\,[a,\,\infty)} \to 0$ when $\delta \to 0$ and $a \to \infty$. Thus, $\left\|z_a^\delta - z^\delta\right\|_{L_2\,[0,\,\infty)} \to 0$ when $\delta \to 0$ and $a \to \infty$.

Consider the case $N = N_a$. Let us estimate the first term:

$$\left\|z_a^\delta - z^\delta\right\|_{L_2\,[0,\,\infty)} \le \frac{1}{\lambda}\left\|\sum_{i=0}^{N-1}(c_i^{a,\delta} - c_i^\delta)\varphi_i - \sum_{i=N}^{\infty} c_i^\delta\varphi_i\right\|_{L_2\,[0,\,\infty)} \le$$
$$\le \frac{1}{\lambda}\left\|\sum_{i=0}^{N-1}(c_i^{a,\delta} - c_i^\delta)\varphi_i\right\|_{L_2\,[0,\,\infty)} + \frac{1}{\lambda}\left\|\sum_{i=N}^{\infty} c_i^\delta\varphi_i\right\|_{L_2\,[0,\,\infty)}. \quad (16)$$

It follows from (10) that $\max\left\{\|\varphi_{n-1}\|_{L_2\,[a,\,\infty)}, \|\varphi_n\|_{L_2\,[a,\,\infty)}\right\}$ is ascendant function of n as $(K_1/\sqrt{n}) \to 0$ while $n \to \infty$. This guarantees the existence of the finite N_a in (11) for the sufficiently large a.

Now we show that the sequence N_a does not have the upper bound when $a \to \infty$. Suppose that this is not the case. Thus

$$\exists\,\overline{N}: \quad \forall\,\overline{a} \quad \exists\,a > \overline{a}: \quad N_a < \overline{N}.$$

Because $\|\varphi_i\|_{L_2\,[a,\,\infty)} \to 0$ when $a \to \infty$ and i is fixed, then for

$$\varepsilon_i = \frac{K_1}{\sqrt{\overline{N}+1}} \quad \exists\,a_i: \quad \forall\,a > a_i \quad \|\varphi_i\|_{L_2\,[a,\,\infty)} \le \frac{K_1}{\sqrt{\overline{N}+1}}.$$

For any $a \ge \max\{a_0,\, a_1,\, \ldots,\, a_{\overline{N}}\}$ we have

$$\|\varphi_i\|_{L_2\,[a,\,\infty)} \le \frac{K_1}{\sqrt{\overline{N}+1}} \qquad \forall\, i = 0, 1, \ldots, \overline{N}.$$

Consequently $N_a > \overline{N}$, and this contradicts to our assumption. Thus $N \to \infty$ when $\delta \to 0$ and $a \to \infty$, and the second term in (16) tends to zero.

Consider the first term:

$$\frac{1}{\lambda}\left\|\sum_{i=0}^{N-1}(c_i^{a,\delta} - c_i^\delta)\varphi_i\right\|_{L_2\,[0,\,\infty)} = \frac{1}{\lambda}\left\|\sum_{i=0}^{N-1}\left(\int_a^\infty u^\delta(\xi)\varphi_i(\xi)\,d\xi\right)\varphi_i\right\|_{L_2\,[0,\,\infty)} =$$
$$= \frac{1}{\lambda}\left[\sum_{i=0}^{N-1}\left(\int_a^\infty u^\delta(\xi)\varphi_i(\xi)\,d\xi\right)^2\right]^{1/2} \le \frac{1}{\lambda}\left[\sum_{i=0}^{N-1}\left(\|\overline{u}\|_{L_2\,[a,\,\infty)}\|\varphi_i\|_{L_2\,[a,\,\infty)}\right)^2\right]^{1/2} \le$$
$$\le \|\overline{u}\|_{L_2\,[a,\,\infty)}\frac{1}{\lambda}\left[N\left(\frac{c_1}{\sqrt{N}}\right)^2\right]^{1/2} = \frac{1}{\lambda}\,c_1\|\overline{u}\|_{L_2\,[a,\,\infty)} \underset{a\to\infty}{\longrightarrow} 0.$$

Hence, the theorem is proved. □

The theorem 3.1 enables us to construct the following algorithm for numerical solution of the problem (3)-(4):

1. Choose the number of the Fourier series terms N according to the formulae (11)-(13).
2. Compute the Fourier coefficients (8) $c_i^{a,\delta}, i = \overline{0,N}$ for the given function u_a^δ.
3. Compute the solution as a partial sum of the Fourier series with the coefficients $d_i^{a,\delta}$ (7).

4 Structure analysis applications of the projection method

Diffraction methods to study the structure of matter with a monochromatic coherent rays (X-rays, electron beams, etc.) measure the diffraction scattering on the object's atoms. At present time various beam types and experimental setups allow to study the structure of both crystalline and non-crystalline solids and liquids. It is also possible to extract the structure of the surface layers.

Under the kinematic approximation of the scattering theory the diffraction pattern acquired by the scattering of coherent monochromatic beam on the potential $p(r)$ is given by [20]:

$$f(s) = K \int p(r) e^{i(sr)}\, dr,$$

where coefficient K depends on the beam type. The measured function $f(s)$ is often called as structure factor.

In the inner regions (that are apart of the surface) of liquid and amorphous systems the scattering potential is radially symmetric, while near the surface the potential is cylindrically symmetric. The corresponding scattering potentials are called radial and cylindrical atomic distribution function respectively.

Due to the symmetry of atom distribution functions in the case of the inner regions we obtain the problem of inversion of the sine-Fourier transform and for the surface layers we have the problem of the Hankel transform inversion. In both cases there are experimental constraints, thus the structure factor can be only measured on a finite interval and it is measured with an experimental error. So we come to the problem statements (5) and (1) respectively.

5 The Sine-Fourier transform

The projection method for the inversion of the sine-Fourier transform (5) with the data given on a finite interval was developed in [11].

The eigenfunctions of the sine-Fourier transform are the odd Hermite functions Φ_n, where

$\Phi_n = e^{-x^2/2} h_{2n+1}(x)$, $\quad h_n(x) = (-1)^n e^{-x^2} \dfrac{d^n e^{-x^2}}{dx^n}$ are the Hermite polynomials.

Using the equivalence for the odd Hermite function norms

$$\|\Phi_n\|^2_{L_2[0,\,R]} = 2n\,\|\Phi_{n-1}\|^2_{L_2[0,\,R]} - \Phi_n(R)\Phi_{n-1}(R),$$

it was shown in [12] that norms $\|\Phi_n\|^2_{L_2[0,\,R]}$ and $\|\Phi_{n+1}\|^2_{L_2[0,\,R]}$ as functions of R intersects even for $R > 1$ (see fig. 1). Nevertheless, the theorem 3.1 can be used as the condition (10) is satisfied for $k = 2$.

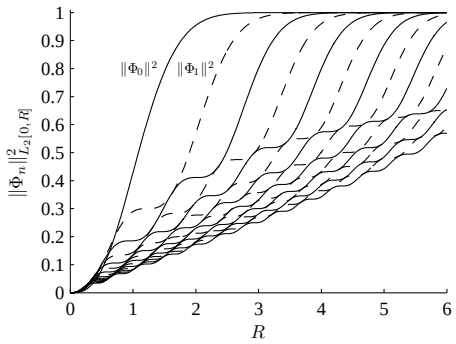

(a)

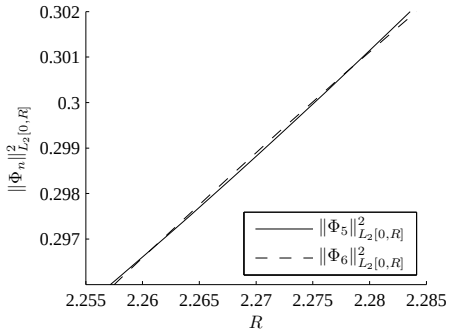

(b)

Рис. 1: (a) Norms of the first 15 odd Hermite functions on interval [0, R]; (b) Intersection of 5-th and 6-th odd Hermite function $L_2[0,\,R]$ norms

6 Zero-order Hankel transform

The justification of the projection method for the zero-order Hankel transform inversion was not done before.

To solve the problem (1) by the projection method we need to prove that eigenfunctions of the Hankel transform meet the requirements of the theorem 3.1.

The zeroth order Laguerre functions are defined as

$$\psi_n(x) = e^{-x/2}L_n(x),$$

where $L_n = \dfrac{1}{n!}e^x\dfrac{d^n}{dx^n}\left(x^n e^{-x}\right)$ are the zeroth order Laguerre polynomials [6].

The Laguerre functions $\psi_n(x)$ are the eigenfunctions of the transform $\tilde{H}$

$$\tilde{H}\left[z\right](t) = \int_0^\infty z(x) J_0(xt)\sqrt{xt}\, dx,$$

which is associated with the Hankel transform

$$H\left[z\right](t) = \frac{1}{\sqrt{t}}\tilde{H}\left[z(x)\sqrt{x}\right].$$

The eigenfunctions of the Hankel transform are [17]:

$$\varphi_n(x) = \sqrt{2x}\,\psi_n(x^2), \tag{17}$$

$$H\left[\varphi_n\right](t) = (-1)^n \varphi_n(t).$$

The examples of the eigenfunctions $\varphi_n(x)$ for $n = 0$, 5, and 10 are given in fig. 2.

This system of functions is full and orthonormal in $L_2\left[0,\,\infty\right)$ and the condition (6) is fulfilled. In this article we prove that $\varphi_n(x)$ can be ordered according to the condition (10).

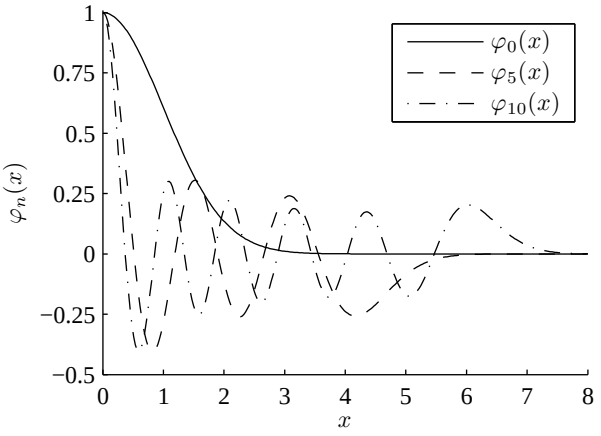

Рис. 2: 0-th (solid line), 5-th (dashed line), 10-th (dash-dotted line) eigenfunctions of the Hankel transform

6.1 Inequality for the norms of the Hankel transform eigenfunctions

Theorem 6.1. *Norms of the eigenfunctions* (17) *of the zero-order Hankel transform satisfy the inequality*

$$\left\|\varphi_n\right\|_{L_2\left[R,\,\infty\right)} \le \left\|\varphi_{n+1}\right\|_{L_2\left[R,\,\infty\right)}, \quad \forall n \in \mathbb{N},\ \forall R > 0. \tag{18}$$

Доказательство. The norms of $\varphi_n(x)$ and the norms of $\psi_n(x)$ are connected as

$$\left\|\varphi_n(x)\right\|^2_{L_2[0,\,R^2]} \;=\; \int_0^{R^2} 2x\psi_n^2(x^2)\, dx \;=\; \int_0^R \psi_n^2(y)\, dy \;=\; \left\|\psi_n(x)\right\|^2_{L_2[0,\,R]},$$

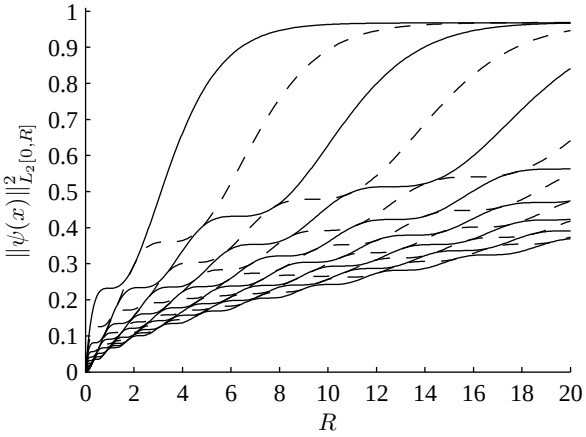

Рис. 3: Norms of the first 15 Laguerre functions $\psi(x)$ on the interval [0, R]

and (18) can be reduced to

$$\|\psi_n(x)\|^2_{L_2[0,\,R]} - \|\psi_{n+1}(x)\|^2_{L_2[0,\,R]} = \int_0^R \psi_n^2(x) - \psi_{n+1}^2(x)\,dx \geq 0. \qquad (19)$$

Consider the derivative of the expression

$$\frac{d}{dx}\left[e^{-x}(L_n(x) - L_{n+1}(x))^2\right] = 2e^{-x}\big(L_n(x) - L_{n+1}(x)\big)\big(L_n'(x) - L_{n+1}'(x)\big) - \\ - e^{-x}(L_n(x) - L_{n+1}(x))^2. \quad (20)$$

Using the relation [6]:

$$L_{n+1}'(x) - L_n'(x) + L_n(x) = 0,$$

the expression (20) can be rewritten as :

$$\frac{d}{dx}\left[e^{-x}\big(L_n(x) - L_{n+1}(x)\big)^2\right] = e^{-x}\big(2L_n^2(x) - 2L_n(x)L_{n+1}(x) - L_n^2(x) + \\ + 2L_n(x)L_{n+1}(x) - L_{n+1}^2\big) = e^{-x}(L_n^2(x) - L_{n+1}^2(x)) = \psi_n^2(x) - \psi_{n+1}^2(x).$$

Thus, we have:

$$\int_0^R \psi_n^2(x) - \psi_{n+1}^2(x)\,dx = e^{-x}\big(L_n(x) - L_{n+1}(x)\big)^2\Big|_0^R = e^{-R}\big(L_n(R) - L_{n+1}(R)\big)^2.$$

It proves the inequality (19) and the theorem. Moreover, the equality is possible only at the points $\hat{R}$, where $L_n(\hat{R}) = L_{n+1}(\hat{R})$. □

The behavior of the norms of the zeroth order Laguerre functions is illustrated in fig. 3

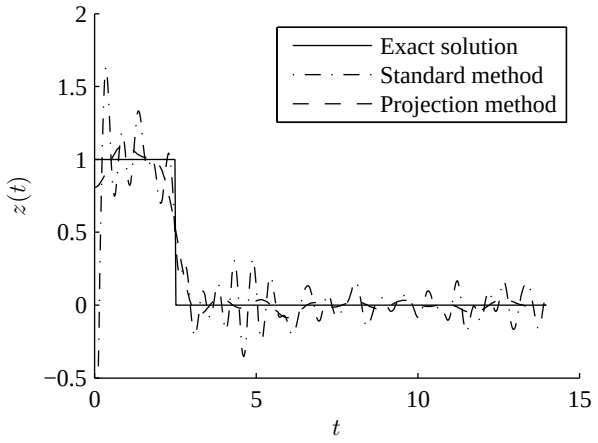

Рис. 4: Reconstruction of model function from $u_{10}^{0,5}$

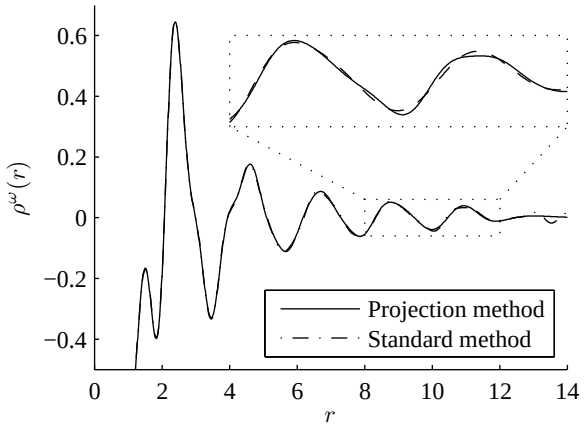

Рис. 5: Reconstruction of model function $z(t) = \frac{1}{2a^2} e^{-t^2/4a^2}$ from $u_{10}^{0,01}$

7 Numerical experiments

7.1 Model function

The projection method gives better results comparing with the "standard method" of the zero-order Hankel transform inversion (zero continuation of the data to the half-line). It can be illustrated with the model function

$$z(t) = H\,[u] = \begin{cases} 1, & t \le 2.5; \\ 0, & t > 2.5. \end{cases}$$

Its zero-order Hankel transform is $u(x) = 2.5 \frac{J_1(2.5x)}{x}$.

To model the real data situation, we added uniformly distributed noise with $\delta = 0.5$ to the function $u(x)$, given on a uniform grid with a step 0.02. The

result for the cutoff value $a = 14$ is shown in fig. 4. The obtained discrepancies for the right part of the equation (3) in this case were 0.89 for the standard method and 0.32 for projectional method.

The number of the functions in the projection method was chosen according to the interval length and the error value. It gave $N = 51$ for $u_{14}^{0.5}$. It can be seen that the use of the "standard method" gave a more oscillating solution comparing with the projection method.

The function $z(t) = \frac{1}{2\sigma^2} e^{-t^2/4\sigma^2}$ with the exact zero-order Hankel transform $u(x) = e^{-\sigma^2 x^2}$ is an illustration of the case of continuous function restoration. In this case we did not have the Gibbs phenomenon so the advantage of the projection method was more clear (see fig. 5). Here we took $\sigma = 2$, $\delta = 0.01$, grid step 0.02 and the cutoff value $a = 10$.

7.2 Computation of cylindrical atomic distribution function

The advantage of the projection method comparing with "standard method" was also shown for the practical problem of computation of the cylindrical atomic distribution function of liquid germanium surface from measured electron diffraction data [21]. The source data was given on the interval [0, 9.8].

The problem

$$H\left[\rho^{\omega}\right](s) = a^{\omega}(s), \tag{21}$$

was solved using the Hankel transform inversion formula with the zero continuation of the experimental data ("standard method") $\rho_{inv}^{\omega}(r)$ and using the projection method (7)-(8) $\rho_{proj}^{\omega}(r)$. In this experiment the noise level was small enough so that $N_\delta > N_a = 34$. The solutions are shown in the fig. 6.

To estimate the quality of the acquired solutions, the experimental structure factor $a^{\omega}(s)$ was recalculated from $\rho_{inv}^{\omega}(r)$ and $\rho_{proj}^{\omega}(r)$ using (21), and the obtained residual norms in L_2 were

$$\left\|a^{\omega}(s) - H\left[\rho_{inv}^{\omega}\right](s)\right\| = 3.49, \quad \left\|a^{\omega}(s) - H\left[\rho_{proj}^{\omega}\right](s)\right\| = 0.40.$$

8 Conclusion

It was illustrated with the zero-order Hankel transform that the projection method is effective for numerical inversion of a wide class of the Fourier integral transforms with the data given on a finite interval. The projection method enables one to take into consideration the length of the given data interval and the value of the data error. It looks promising to construct fast implementations of projection methods by analogy with the fast Hermite projection method [10].

Acknowledgements

The work was supported by the federal target program "Scientific and scientific-pedagogical personnel of innovative Russia" in 2009-2013 and RFBR grant 10-01-00535.

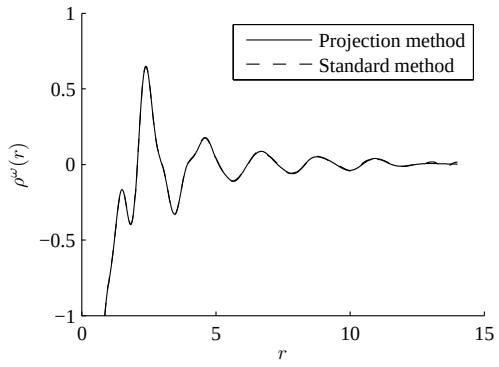

(a)

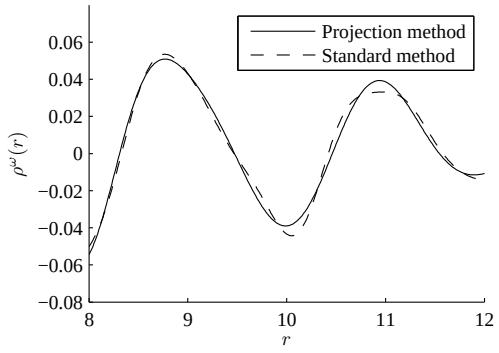

(b)

Рис. 6: (a) Cylindrical atomic distribution function $\rho^{\omega}(r)$ of liquid germanium, calculated by the "standard method" and projection method; (b) Zoomed fragment

Список литературы

[1] Li Yu, M. Huang, M. Chen, W. Huang, and Z. Zhu. Quasi-discrete Hankel transform. *Optics Letters*, 23(6):409–411, 1998.

[2] M. El-Shahed and M. Shawkey. Generalized finite Hankel transform. *Integral Transforms and Special Functions*, 17:39–44, 2006.

[3] D. R. Mook. An algorithm for numerical evaluation of Hankel and Abel transform. *IEEE Transactions on Acoustics, Speech and Signal Processing*, 31(4):979–985, 1983.

[4] V. F. Uhov, N. A. Vatolin, B. R. Gel'chinskiy, V.P. Beskachko, and O. A. Esin. *Interparticle interaction in melted metals.* Nauka, Moscow, 1979. (In Russian).

[5] P. C. Shah and R. K. M. Thambynayagam. Application of the finite Hankel transform to a diffusion problem without azimuthal symmetry. *Transport in Porous Media*, 14(3):247–264, 2003.

[6] G. Szogö. *Orthogonal Polynomials.* American Mathematical Society, New York, 1939.

[7] V. Magni, G. Cerullo, and De Silvestri. High-accuracy fast Hankel transform for optical beam propagation. *J. Opt. Soc. Am. A*, 9(11):2031–2033, 1992.

[8] V. V. Vasin and A. N. Ageev. *Ill-posed problems with a priori information.* Nauka, Ekaterinburg, 1993. (In Russian).

[9] N. T. Eldabe, M. El-Shahed, and M. Shawkey. An extension of the finite Hankel transform. *Applied Mathematics and Computation*, 151:713—717, 2004.

[10] A. S. Krylov and D. N Korchagin. Fast Hermite Projection Method. *Lecture Notes in Computer Science*, 4141:329–338, 2006.

[11] A. S. Krylov and A. V. Liakishev. Numerical Projection Method For Inverse Fourier Transform and its Application. *Numerical Functional Analysis and optimization*, 21:205–216, 2000.

[12] A. S. Krylov and A. V. Liakishev. Inequality for Hermite function norms on finite interval. *Vestnik Moskovskogo Universiteta*, 1:17–19, 1999. (In Russian).

[13] A.S. Krylov and A.V. Vvedenskii. Software Package for Radial Distribution Function Calculation. *Journal of Non-Crystalline Solids*, 192:683–687, 1995.

[14] M. Mizotin, A. Krylov, and M. Spiridonov. Application of projection method for analysis of structural dependencies in surface layers of melts. *Rasplavy*, 5:18–26, 2009.

[15] I. N. Sneddon. On finite Hankel transforms. *Philosophical Magazine*, 7:17–25, 1946.

[16] W. E. Higgins and D. C. Munson. A Hankel transform approach to tomographic image reconstruction. *IEEE Transactions on Medical Imaging*, 7(1):59–72, 1988.

[17] Arthur Erdelyi, editor. *Tables of Integral Transforms*, volume 2. McGraw-Hill, New York, 1954.

[18] E. C. Cavanagh and B. D. Cook. Numerical evaluation of Hankel Transform via Gaussian-Laguerre polynomial expressions. *IEEE Transactions on Acoustics, Speech and Signal Processing*, 27:361–366, 1979.

[19] G. M. Zhidomirov, editor. *X-ray spectral method of studying amorphous objects structure: EXAFS spectroscopy.* Nauka, Novosibirsk, 1988. (In Russian).

[20] B. K. Veinshtein. *Structural electronography.* Academy of sciences, Moscow, 1956. (In Russian).

[21] M. A. Spiridonov, A.V. Lavrov, and S. I. Popel. Atomic ordering in surface layers of cuprum-germanium melts. *Metals*, 2(3):49–53, 1990. (In Russian).